JOURNAL OF MATERIALS SCIENCE 35 (2000) 2973–2984

Tensile behavior of SiC/C and Rene'41 following isothermal exposure and thermal fatigue

J. L. PIERCE*, L. P. ZAWADA
Materials, Manufacturing, and NDE Directorate, Air Force Research Laboratories, Wright-Patterson Air Force Base, Ohio 45417, USA

R. SRINIVASAN
Mechanical and Materials Engineering Department, Wright State University, Dayton, Ohio 45435, USA
E-mail: pierce@udri.udayton.edu

The performance of a coated silicon carbide/carbon composite under isothermal and thermal fatigue conditions was investigated. The material studied is known as Ceracarb™ which consists of eight-harness satin weave Nicalon® silicon carbide cloth reinforcement, a carbonaceous matrix, and a silicon carbide composite coating. This advanced composite is being considered for replacing the nickel based superalloy Rene'41, as the exhaust nozzle components on military afterburning turbine engines. Thermal fatigue experiments, performed in the laboratory using a thermal cycling test system, were intended to roughly simulate the thermal excursions of an afterburning exhaust nozzle. Several thermal profiles were used to characterize the role of temperature, number of cycles, temperature range, and time at temperature, on the room temperature residual tensile strength of the material. The same thermal profiles were also conducted on test specimens of Rene'41 in order to compare its durability in the laboratory simulation test set-up to the composite. Both materials showed no loss in strength from the as-received condition following thermal testing. However, the Rene'41 showed evidence of microstructural instability at the maximum test temperature of 1093°C (2000°F) which did affect the toughness of the material. While the results from this study showed that both materials retained strength when thermally exposed in the laboratory under no loads, thermal testing under load may provide a more realistic view of how the materials perform in the afterburning exhaust nozzle application.

1. Introduction

The need for greater efficiencies and higher thrust-to-weight ratio's in military turbine engines drives both the development of advanced materials and the test techniques required to evaluate their behavior. Materials that have greater strength-to-weight ratios and can operate at significantly higher temperatures will provide for significant improvements in the performance of advanced turbine engines. Ceramic matrix composites (CMCs) are an emerging class of materials which have shown potential for replacing currently used high-temperature nickel-based superalloys (SAs) in certain turbine engine applications, particularly those with demanding thermal environments [1–5]. Conventional nickel-based superalloys have lower specific properties and can severely degrade at elevated temperatures. CMCs have low densities and retain strength and stiffness at temperatures in excess of 1000°C (1800°F) [1, 2, 6]. However, these materials are not as well understood as their metal predecessors.

A promising application for CMCs is in the afterburner of military turbine engines. Conditions in the afterburning section of a turbine engine require materials which must withstand extreme temperatures (>1000°C), as well as rapid thermal cycles, while maintaining basic strength requirements [1, 4, 5, 7–11]. Nickel-based superalloys, such as Rene'41, are typically used for the divergent seal and flap components which make-up the exhaust nozzle in military turbine engines. However, seals and flaps made from Rene'41 have been shown to crack extensively under the extreme afterburning conditions [11, 12], illustrating a need for more durable materials in the application [13].

An example of the cracking experienced by the exhaust nozzle components during service on a military afterburning engine is given in Fig. 1. Pictured in the figure are two divergent seals on either side of a divergent flap. These parts are from an F110 engine that was mounted on a F16 Fighter. Extensive cracking in these components, such as shown in the figure, cause

* *Present Address*: Structural Integrity Division, University of Dayton Research Institute, Dayton, Ohio, 45411, USA.

Figure 1 A photograph of a GE-F110-100 exhaust nozzle divergent flap and two divergent seals that have been removed from service due to severe cracking. The Rene'41 components suffer from extensive creep deformation and cracking due to the environment.

expensive parts replacement, excessive vehicle downtime, and significant labor efforts.

Cracking in the metal seals and flaps are a result of the severe thermal environment. During operation, stresses develop as a result of pressure differentials, thermal gradients, and physical constraints on the components. These stresses in combination with a steep loss in tensile strength and lowered creep resistance at temperatures above 700° [9, 10, 14–16], allows for the damage to occur.

Despite their potential, the use of CMCs in aerospace applications may be limited by their long-term oxidation resistance. Fibers used in many structural CMCs, such as silicon carbide, can degrade during extended use above 1000°C in oxygen containing environments [2, 6, 7, 10, 17]. Typical fiber coatings and fiber/matrix interphase materials such as carbon and boron nitride, chosen for their crack deflection capability, are susceptible to oxidation at even lower temperatures [2, 6, 18–20]. The surrounding matrix material in many composites can contain constituents that are oxygen sensitive at elevated temperatures as well. Selective oxidation of the matrix can leave voids that can allow for further environmental attack of the underlying fibers. In some cases, matrix materials contain open porosity and/or a high density of cracks that result from processing or loading which can also allow ingress of oxygen. Long-term exposure of resin based inhibited matrix materials at what are considered intermediate temperatures (600 to 900°C) [18, 19, 21] can also allow for oxidation ingress. In this temperature range glassy phases relied upon for oxidation protection have a high viscosity and leave the material susceptible to embrittlement due to oxidation.

An approach to enhance the oxidation resistance of CMCs is the use of external composite coatings. These coatings are usually comprised of traditional materials such as silicon carbide and can be applied by several techniques. However, there is usually a large difference in the coefficient of thermal expansion (CTE) between the substrate and the exterior coating material. Cracking and spallation of the coating will occur if the thermal expansion mismatch is large, leaving inadequate protection for the substrate. Since CMCs will see both high temperatures and rapid thermal fluctuations when utilized as exhaust nozzle and other hot section components, CTE mismatch with the coating material is a major concern.

One particular CMC, namely silicon carbide fiber-reinforced carbon (SiC/C), has shown excellent

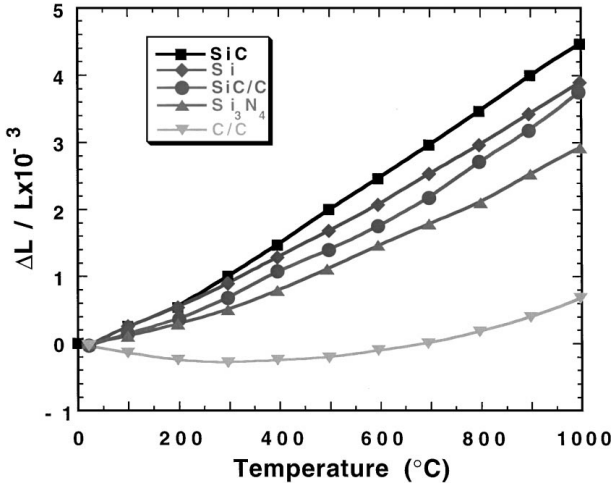

Figure 2 A comparison of the thermal strains measured for SiC/C and C/C relative to several coating materials: SiC, Si, and Si_3N_4 [22].

strength and durability at elevated temperatures [2, 6, 22, 23]. Due to its carbon matrix, this material relies heavily on an exterior silicon carbide coating to prevent oxidation at elevated temperatures. The high temperature durability of SiC/C is attributed to the relatively low CTE mismatch between the composite and the exterior coating. Fig. 2 shows a plot presented by S. C. Schwartz *et al.* [22] that compares the thermal strain obtained at different temperatures up to 1000°C for both C/C and SiC/C relative to SiC, Si, and Si_3N_4 coating materials. The figure shows that the thermal strain experienced by SiC/C is closer to the thermal strain measured for the coating materials then that experienced by C/C.

Due to the attractive qualities and potential end-use, it was the intent of this study to evaluate the high temperature performance of a coated SiC/C material with respect to the requirements for a military afterburning turbine engine exhaust nozzle application and to compare the results to the baseline exhaust nozzle component material, Rene'41. Laboratory tests were performed on both SiC/C and on Rene'41 using a thermal cycling system comprised of a tube furnace with a computer controlled pneumatic actuator to roughly simulate the thermal excursions of an exhaust nozzle on an afterburning turbine engine. Variations of the thermal fatigue tests were performed to address the role of the maximum temperature, the range of temperature variation, the number of cycles, and the time at temperature on the durability of the materials. The thermally tested specimens were evaluated through comparison of the room temperature residual strengths against as-received material in each case.

2. Material

2.1. General description

Two different materials were tested in this study: a ceramic matrix composite and a nickel based superalloy. The CMC material tested is a coated silicon carbide fiber-reinforced carbon (SiC/C) manufactured by the former Hitco Technologies under the trademark name Ceracarb™ SC537EH. (For all further discussion, the material will be referred to as "Ceracarb™"). Continuous nanocrystalline ceramic grade NICALON® silicon carbide fiber reinforces the composite. These fibers are woven in a balanced 8-harness satin weave cloth. The cloth is stacked in a 0/90 sequence, for a total of twelve plies. This composite architecture is the same as the one considered for use in exhaust nozzle application. The matrix is primarily resin based inhibited pyrolitic carbon and a filler. After the pyrolysis process, there is extensive shrinkage as the resin is converted to carbon. Therefore, the composite is further densified by chemical vapor infiltration (CVI) of additional carbon. The bulk density of the test material was measured to be 2.12 g/cc, and the fiber volume fraction was measured to be 38.8 ± 8.2%.

This material utilizes a multi-layered protection scheme. Parts of the inhibited matrix form a protective glassy phase when exposed to oxygen at temperatures in excess of 800°C (1472°F) [22, 23]. In addition, the entire composite structure is coated with an exterior protective coating and a seal coating. The underlying exterior coating layer is silicon carbide (Chromalloy RT42). The material is applied by chemical vapor deposition (CVD) to the substrate and provides protection up to 1371°C (2500°F) [22]. A M185A glaze coating is then applied over the silicon carbide. The glaze coating has a relatively low melting temperature and acts to seal cracks in the preliminary coating.

All of the major components which make up the Ceracarb™ material can be viewed in Fig. 3. A typical transverse cross section of the as-received illustrates the 0° and 90° fibers, the matrix, the dual exterior coating systems, and the matrix cracks that develop during processing (Fig. 3a). At higher magnification, the various constituents which make-up the matrix in the Ceracarb™ can be seen (Fig. 3b). There is a the large fraction of filler materials within the pyrolyzed carbon matrix which are responsible for the protective glassy phase formation at temperature [22, 23]. Sometimes layers of carbon around fibers and around shrinkage cracks are evident (Fig. 3b). These carbon layers are formed during the densification of the composite through CVI of additional carbon.

The nickel based superalloy tested, Rene'41, is the material currently used for exhaust nozzle seals and flaps in several engine families. Test material for this study was cold rolled to the same approximate thickness as used for the exhaust components. The alloy composition was primarily nickel with the balance being as shown in Table I. Nominal values for the composition are shown in percent by weight. Material processing included a solutionization at 1080°C (1975°F) followed by water quenching. The resultant microstructure can be described as having an ASTM grain size of 7 to 8 and uniformly dispersed carbides. Fig. 4 shows a micrograph of the as-received microstructure. The bulk density of the test material was approximately 8.2 g/cc (0.286 lb/in^3).

2.2. Specimen geometry

Ceracarb™ test specimens received for this study were 152 mm long dogbone specimens. The dimensions of

TABLE I The manufacturers composition (wt%) of the Rene'41 tested

Cr	Co	Mo	Ti	Fe	Al	C	Mn	Si	Cu	Zr	B	S
19.18	10.43	9.40	3.23	2.42	1.56	0.088	0.06	0.04	0.04	0.037	0.006	.002

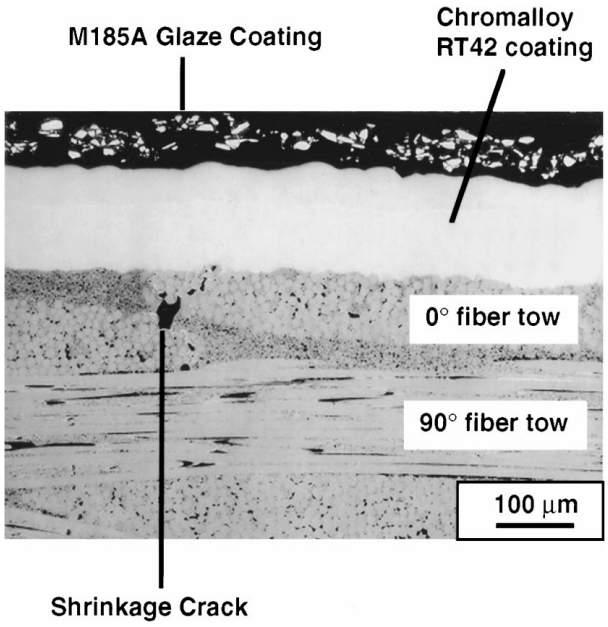

Figure 3 The general microstructure of Ceracarb^{TM} SC537EH material as manufactured by HITCO Technologies Inc.: (a) low magnification optical micrograph which illustrates the 0° and 90° fibers, the matrix, the dual exterior coating systems, and the matrix cracks that can develop during processing, and (b) high magnification optical micrograph depicting individual fibers, filler particles in the carbon matrix, a shrinkage crack, and layers of the CVI pyrolitic carbon.

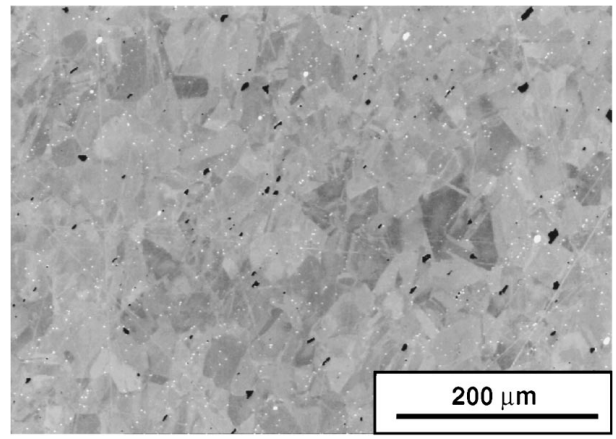

Figure 4 SEM micrograph taken at 200× which shows the general microstructure of the nickel-based superalloy Rene'41 in the as-received condition: solutionized at 1080°C (1975°F), water quenched, and cold rolled. The specimen was prepared using a chromate electropolish.

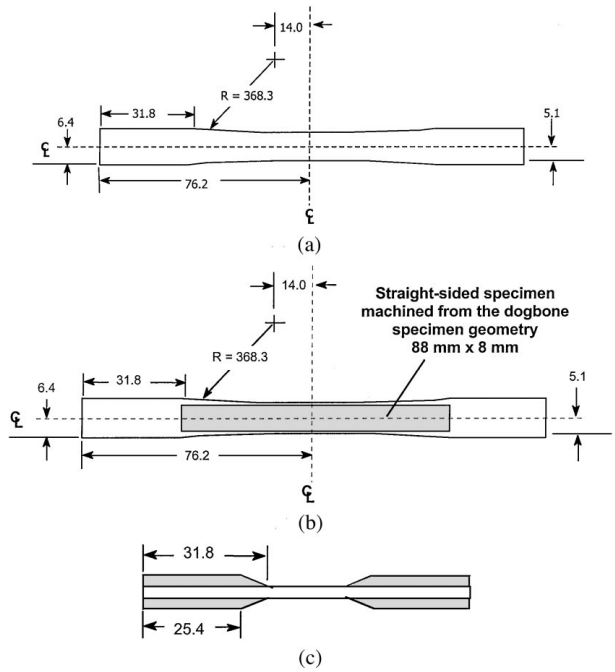

Figure 5 Schematics of the Ceracarb^{TM} test specimens: (a) the original dogbone test specimen geometry utilized for all of the thermal testing, (b) the straight-sided test specimen geometry machined from the dogbone specimen used for all of the room temperature tension tests, and (c) the straight-sided test specimen with the ends tabbed according to the technique for face-loaded ceramic composites [24].

the dogbone specimens are shown in Fig. 5a. This geometry was used for thermal testing in order to utilize the material's as-fabricated coating system. Following thermal treatment, the dogbone test specimens were machined into 88 mm by 8 mm straight sided coupons for room temperature residual strength testing (Fig. 5b). The straight-sided geometry was preferred over the dogbone geometry for residual strength testing. Additional work was planned in which actual engine tested components would be obtained, machined into straight-sided coupons, and then tested for residual strength for comparison. These straight-sided machined test specimens would only have the exterior coating on the top and bottom surfaces which would allow for a direct one-to-one comparison to test specimens machined from engine tested hardware. In addition, the length machined off of the dogbone specimens eliminated the material which was gripped during

pre-conditioning fatigue. Pre-conditioning fatigue testing is discussed in the Experimental Procedure section.

As-received tensile tests performed on the Ceracarb^{TM} material were conducted on test specimens with the same straight-sided geometry as described above. Both the as-received and residual strength test specimens were prepared by tabbing each end with fiberglass tabs according to the technique for face-loaded ceramic composites [24] before testing. Fig. 5c provides a schematic illustration of a straight-sided tensile specimen with tabs.

All of the tests conducted on Rene'41 were performed using a dogbone test specimen geometry. Test specimens were machined from the rolled sheet by electro-discharge machining (EDM), and the edges were polished. The specimen dimensions are shown in Fig. 6. As-received and thermally tested material was tension tested in the originally machined dogbone geometry.

3. Experimental procedure

Evaluation of the Ceracarb^{TM} and the Rene'41 was based on a comparison of the room temperature tensile strengths obtained from thermally treated material against as-received material. The flow chart in Fig. 7 provides a pictorial overview of the testing scheme. Test specimens of Ceracarb^{TM} and Rene'41 were first tension tested in the as-received condition to provide baseline strengths for each material. Other test specimens from both materials were then subjected to either isothermal heat treatment or thermal

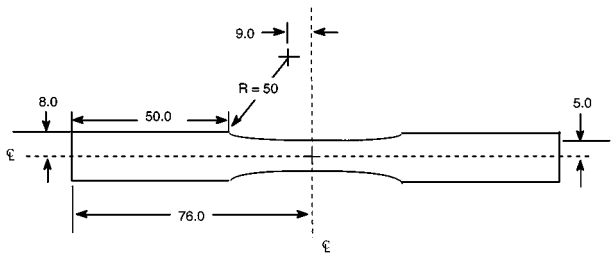

Figure 6 Schematic of the Rene'41 dogbone test specimen geometry utilized for all testing.

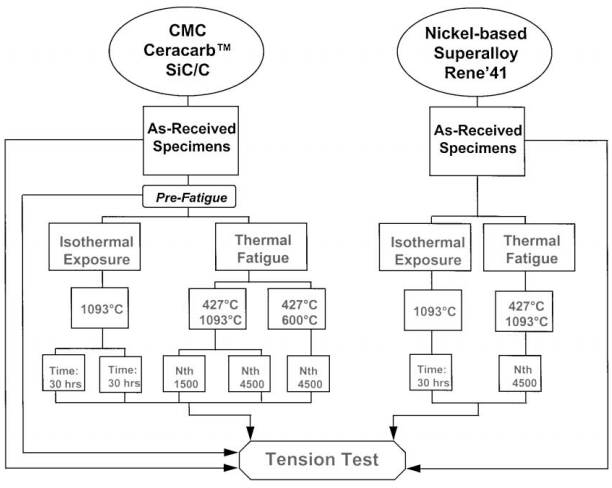

Figure 7 Pictorial overview of the testing scheme for both the Ceracarb^{TM} material and the Rene'41.

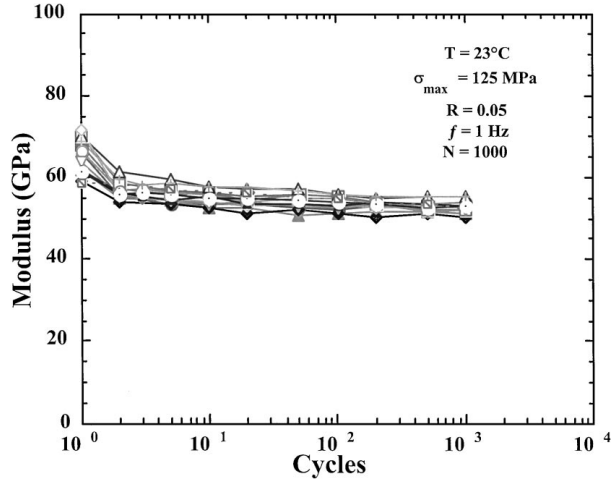

Figure 8 Plot of modulus versus cycles for Ceracarb^{TM} test specimens pre-conditioned in fatigue at room temperature. The difference in modulus was 14 MPa on the first cycle and decreased to within 5 MPa after 1000 cycles.

fatigue. Several thermal profiles were used to characterize the role of time at temperature, cycle count, maximum temperature, and/or ΔT on the room temperature residual strength of the materials. In the case of the Ceracarb^{TM} material, all of the test specimens were first pre-conditioned using mechanical fatigue testing before undergoing thermal treatment. A number of these mechanically fatigued test specimens were set aside without subsequent thermal treatment to be residual strength tested for comparison purposes. The Rene'41 material, which was not pre-conditioned, saw only the most extreme isothermal exposure and thermal fatigue conditions. The thermally treated specimens from both materials were then tested for residual strength and compared against the respective as-received material.

Ceracarb^{TM} test specimens that were thermally treated were first subjected to mechanical fatigue, which are referred to as pre-conditioning fatigue in the following. The pre-conditioning fatigue was performed in an attempt to normalize the condition of each test specimen by increasing the density of matrix cracks and to promote the effects of oxidation by introducing cracks in the exterior coating. These tests were run at room temperature on as-received material in the dogbone specimen geometry using an MTS† horizontal servo-hydraulic test machine with rigid hydraulic clamping grips. Test specimens were fatigued at a maximum stress of 125 MPa for 1000 cycles at room temperature with a load ratio of 0.05 and a frequency of 1 Hz. A stress of 125 MPa was selected as it is above the proportional limit of the Ceracarb^{TM} material [4, 5, 22, 23]. The effects of pre-conditioning fatigue are illustrated by the modulus vs. cycle plot in Fig. 8. The plot shows that the largest variation in modulus from specimen to specimen is greater than 10 GPa on the first cycle. After the first cycle, the moduli values drop considerably and then appear to remain fairly constant for the last few hundred cycles. On the last cycle, the scatter in the moduli from specimen to specimen is within

† MTS is a trademark of MTS Systems Corporation, Minneapolis, MN.

5 GPa. The initial drop in modulus is representative of an increase in the matrix crack density. The consistency in the moduli from specimen to specimen near the last cycle may illustrate that a saturation level of matrix cracking for the given stress has been achieved.

Following pre-conditioning fatigue, some of the Ceracarb^{TM} test specimens were heat treated and others were thermally fatigued. Heat treatment was performed at 1093°C using a box furnace. The furnace temperature used was comparable to the maximum temperature experienced by components in the afterburning section of an engine during afterburner ignition at maximum power [1, 3, 7–10]. A number of the Ceracarb^{TM} test specimens were exposed to temperature for ten hours while others were exposed for thirty hours to characterize the role of time at temperature on the residual strength. The Rene'41 specimens were exposed to the more severe condition of 1093°C for thirty hours.

The thermal fatigue tests were performed using a resistance heated tube furnace with a computer controlled in-line pneumatic actuator to insert and retract test specimens from the furnace hot zone. A photograph of the thermal fatigue test system used is given in Fig. 9a. The test specimens were attached to an alumina rod which extended from the pneumatic cylinder ram. Wire ties were used to attach the test specimens to the alumina rod, but were only used in the tab section of each sample. Fig. 9b provides an illustration of the Ceracarb^{TM} specimen test set-up. The Rene'41 test specimens required additional wire ties as well as an extra support rod, as shown in Fig. 9c. Additional wire ties and support were needed as the wire would creep at temperature under the weight of the SA metal.

The end of an S-type thermocouple, housed in a thin alumina tube, was placed near the middle of each test specimen for temperature measurement. The thermocouple output was used to position the test specimen in and out of the furnace according to the programmed temperature profile. A single thermal fatigue cycle involved inserting the test specimen into the furnace, holding it there until it reached the programmed temperature, and then retracting it from the furnace. A small fan was utilized to speed up the cooling rate.

Ceracarb^{TM} specimens were cycled between a minimum temperature of 427°C (800°F) and a maximum temperature of either 1093°C (2000°F) or 600°C (1112°F) in order to characterize the role of maximum temperature and ΔT on the residual strength. The initial thermal cycle range was between 427 and 1093°C, which was to simulate afterburner ignition. Several test specimens were thermally fatigued for 1500 cycles, simulating 1500 afterburner lights. Other test specimens were thermally fatigued for three times the number of cycles (4500 cycles) to look at the effects of cycle count on residual strength. A third set of Ceracarb^{TM} specimens were thermally cycled between intermediate temperatures, 427 and 600°C, for 4500 cycles. The Rene'41 material was subjected to thermal fatigue only under the most severe conditions, between temperatures of 427 and 1093°C for 4500 cycles.

Tension tests on both Ceracarb^{TM} and Rene'41 materials were performed using a vertical servo-hydraulic test machine mounted with wedge grips and serrated grip inserts. A photograph of the testing apparatus described above is shown in Fig. 10. Tension tests were performed on both materials in the as-received, pre- conditioned, and thermally treated conditions with this set-up. All tests were run at room temperature and with a constant testing rate of 0.05 mm/s. A clip-gage extensometer was used for strain measurement.

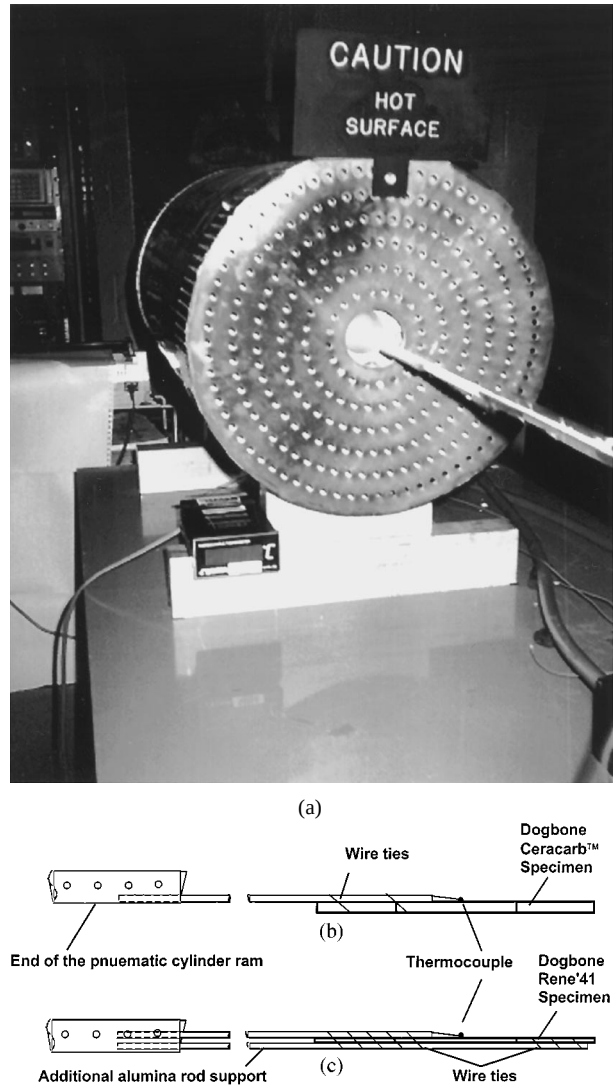

Figure 9 Illustrations of the thermal fatigue test set-up: (a) photograph of the thermal cycling test system used, (b) schematic representation of the Ceracarb^{TM} test specimen set-up showing the limited number of wire ties used, and (c) schematic representation of the Rene'41 test specimen set-up showing the extra wire ties and the additional rod for support.

4. Results

4.1. Ceracarb^{TM} (SiC/C)

As-received tensile properties as well as residual strength results for the Ceracarb^{TM} material tested are presented in Table II. The as-received tensile behavior is depicted by the stress-strain curves shown in Fig. 11. The average strength, modulus, and strain at failure for the as-received material was found to be approximately 185 MPa, 76 GPa, and 0.36%, respectively. Each curve in the figure shows a non-linear stress strain response from the onset of loading which is associated with matrix cracking and interfacial debonding. At a point

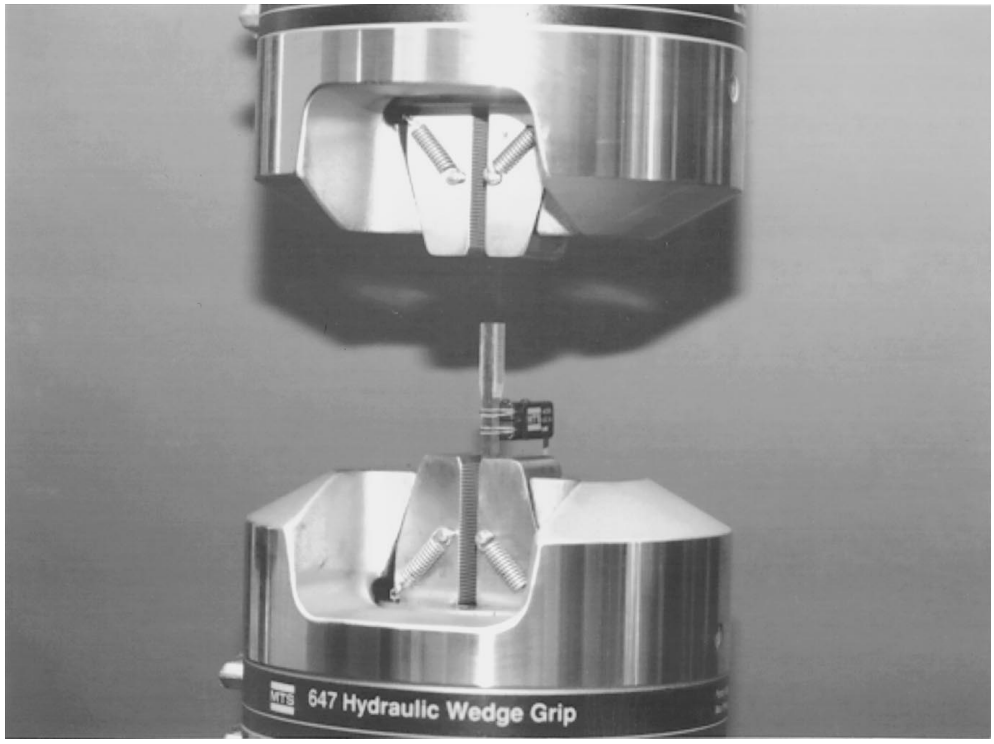

Figure 10 Photograph of the testing apparatus used for all tensile testing. Also shown is a tabbed Ceracarb™ test specimen mounted with a clip-gage extensometer.

TABLE II Tensile results from as-received and thermally treated Ceracarb™ material

Ceracarb™

Specimen#/test type	UTS (MPa)	Modulus (GPa)	Strain @ fail (%)
As-received			
94-375	194	76	0.35
94-376	171	83	0.33
94-394	194	68	0.40
94-395	182	—	—
Pre-fatigue			
94-363	185	60	0.33
94-394B	206	62	0.38
94-362	162	65	0.40
Isothermal-10 hrs			
94-380	193	60	0.35
94-381	194	58	0.37
94-382	189	58	0.35
Thermal fatigue (Tmax = 1093 C, N = 1500)			
94-383	195	57	—
94-384	189	59	0.37
94-385	195	55	0.39
Isothermal—30 hrs			
94-387	222	60	0.42
94-388	200	60	0.35
Thermal fatigue (Tmax = 1093 C, N = 4500)			
94-371	205	51	0.44
94-372	183	61	0.31
Thermal fatigue (Tmax = 600 C, N = 4500)			
94-352	177	59	0.37
94-365	179	58	0.39

above approximately 0.1% strain (about 100 MPa) in each curve, the stress-strain response becomes approximately linear with a lower tangential modulus. This suggests that above 100 MPa the matrix of the composite had become sufficiently damaged to cause the load to transfer to the fibers.

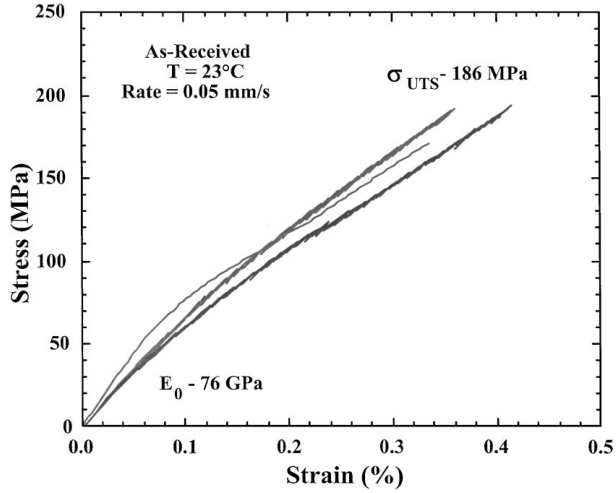

Figure 11 Stress vs. strain traces for as-received Ceracarb™ tested at room temperature.

The stress-strain curves for the Ceracarb™ test specimens that first underwent pre-conditioning fatigue and were subsequently tension tested are plotted in Fig. 12. These tests were performed to determine if the mechanical fatigue had an influence on the strength of the material. The average strength and modulus for the three specimens tested were approximately 184 MPa and 63 GPa, respectively. A comparison of the as-received strength and that following pre-conditioning fatigue shows that the mechanical fatigue cycles had no effect on the strength of the composite. There is an effect from the pre-conditioning fatigue on the modulus and the overall shape of the stress-strain response. The average modulus for the pre-fatigued material was

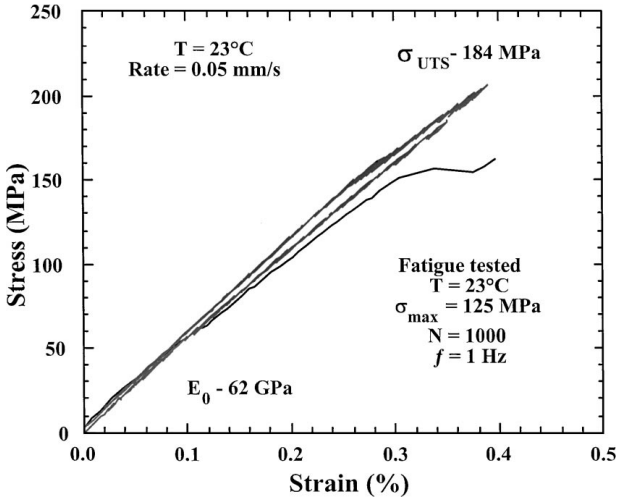

Figure 12 Stress vs. strain traces for Ceracarb™ material which had been previously pre-fatigued under tension-tension cyclic loading to maximum stress of 125 MPa for 1000 cycles.

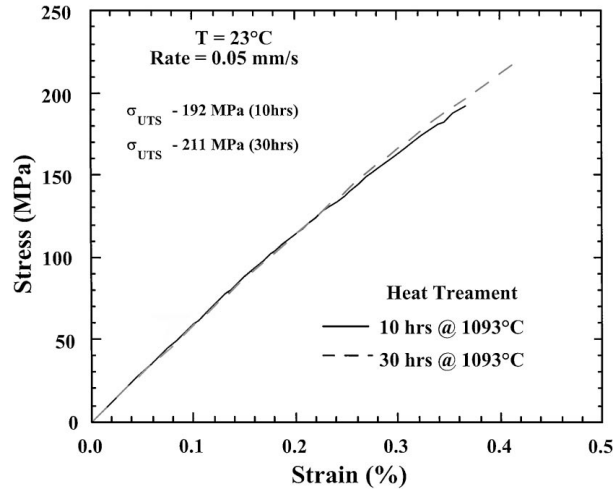

Figure 13 Representative stress vs. strain traces for Ceracarb™ material which had been pre-fatigued and heat treated for 10 to 30 hours at 1093°C.

approximately 9 GPa lower than for the as-received material. This result was consistent with the difference in modulus measured during the pre-conditioning fatigue tests between cycle one and cycle 1000 shown in Fig. 8. The stress-strain curves for the pre-conditioned specimens show linear behavior from the onset of loading to a point above the pre-conditioning stress level of 125 MPa, whereas the as-received material showed non-linear behavior. The change in the stress-strain response is explained by the increase in the amount of matrix cracking induced by the fatigue testing.

The test specimens which were heat treated for either ten or thirty hours showed no loss in strength compared to the as-received material. Average strength and modulus measured for the specimens exposed for ten hours were 192 MPa and 59 GPa, respectively. The average strength of the material exposed for thirty hours was 211 MPa and the average modulus was 57 GPa. From these data, it appears that neither of the isothermal exposure conditions were detrimental to the retained strength. The drop in modulus observed for both heat treat conditions compared to as-received material was similar to that seen in the non-exposed pre-conditioned material. The stress-strain behavior of material heat treated for either 10 hours or 30 hours is nearly identical, although the strength of the material heat treated for 30 hours is slightly higher. A representative stress-strain curve from both the exposures can be found in Fig. 13. The stress-strain behavior is the same as described for the pre-conditioned material, the response is linear from the onset of loading, up to the pre-conditioning fatigue stress level of 125 MPa.

The average residual strength of the specimens tested under thermal fatigue conditions between 427°C and 1093°C for 1500 cycles and those tested for 4500 cycles in the same temperature range also showed no loss in strength compared to the as-received material. The average strengths measured for the two conditions were 193 MPa and 194 MPa, respectively. Test specimens thermally fatigued between 427°C and 600°C for 4500 cycles had a slightly lower retained strength than the as-received material at 178 MPa. Representative tensile

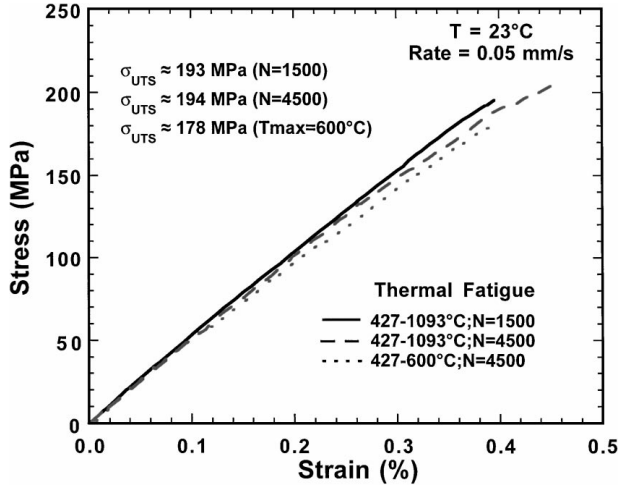

Figure 14 Representative stress vs. strain traces for Ceracarb™ material which had been pre-fatigued and subsequently thermally fatigued between 427°C and 1093°C for 1500 cycles and 4500 cycles and also from 427°C to 600°C for 4500 cycles.

curves generated from specimens tested under the various thermal fatigue conditions are shown in Fig. 14. The stress-strain response was found to be similar to that observed for the pre-conditioned and the heat treated test specimens.

Data obtained from the laboratory tested Ceracarb™ specimens suggests that the CMC material suffers no loss in strength from the as-received condition, even after being subjected to extreme thermal conditions. This observation is exemplified in the bar chart shown in Fig. 15. In the figure the dots represent the mean value of tensile strength for each test condition. In all cases, except for the material heat treated for 30 hours at 1093°C and that thermally fatigued between 427°C and 600° C, the mean strength values are approximately equal to the as-received tensile strength.

It appears from Fig. 15 that the 30 hour heat treatment may have caused an increase in strength. Although no mechanism for the observed increase in strength after the longer heat treatment can be given at this time, the phenomenon of increased strength at

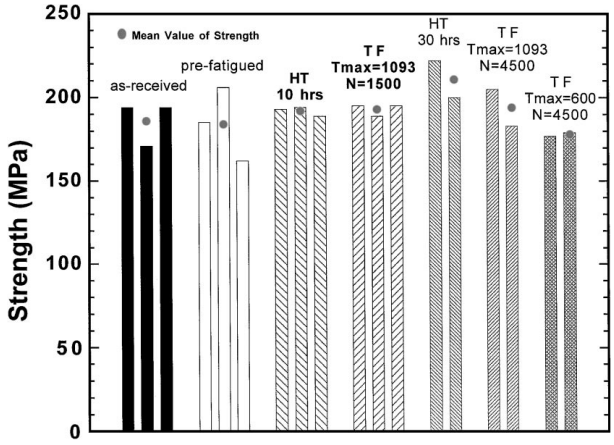

Figure 15 Bar chart comparing the ultimate tensile strengths measured for the Ceracarb^{TM} material at each test condition. Shown from left to right are data from as-received, pre-fatigued, heat treated at 1093° for 10 hours, thermally fatigued between 427 and 1093° for 1500 cycles, heat treated at 1093°C for 30 hours, thermally fatigued between 427 and 1093°C for 4500 cycles, and thermally fatigued materials between 427 and 600°C for 4500 cycles, respectively. The dots represent the average strength.

high temperature has been demonstrated for various CMCs in the past. Lara-Curzio *et al*. [25] present fatigue data for a polymer-derived CMC with woven Nicalon® fibers where the peak stress on the first cycle was greater at 982°C and 1204°C than it was for 25°C. However, in this case the strength increase was noted during testing at temperature and does not necessarily pertain to retained strength at room temperature. Recent testing by Lee *et al*. [26] has shown that a fiber-reinforced oxide/oxide CMC tested in fatigue at 1100°C for 100,000 cycles at 150 MPa exhibited retained strength at room temperature that was 24% higher than the as-received room temperature strength. In this case the change in the residual stress state was attributed to a decreased number of stress concentration sites within the composite due to the fatigue cycling and no mechanism relating to the temperature was speculated.

The test specimens thermally fatigued between 427°C and 600°C were expected to show a loss in strength as a result of intermediate temperature embrittlement. In this temperature range, the sealant materials do not readily flow and seal cracks to guard against oxidation [18, 19, 21]. These conditions were deemed important to study as the exhaust components are exposed to these intermediate temperatures for a large percentage of operation time. The average strength for those specimens tested to 600°C was the lowest of any of the conditions tested in this study, but the difference in behavior compared to the as-received material does not appear to be significant.

The results which show that there was essentially no loss in strength due to pre-conditioning fatigue testing alone or with subsequent thermal testing suggests that no significant damage was incurred to the fibers in either case. Most fiber-dominated composite materials show a change in strength as a result of a significant number of fibers damaged by mechanical or oxidative conditions. However, no significant changes in strength were measured in the material under the conditions tested.

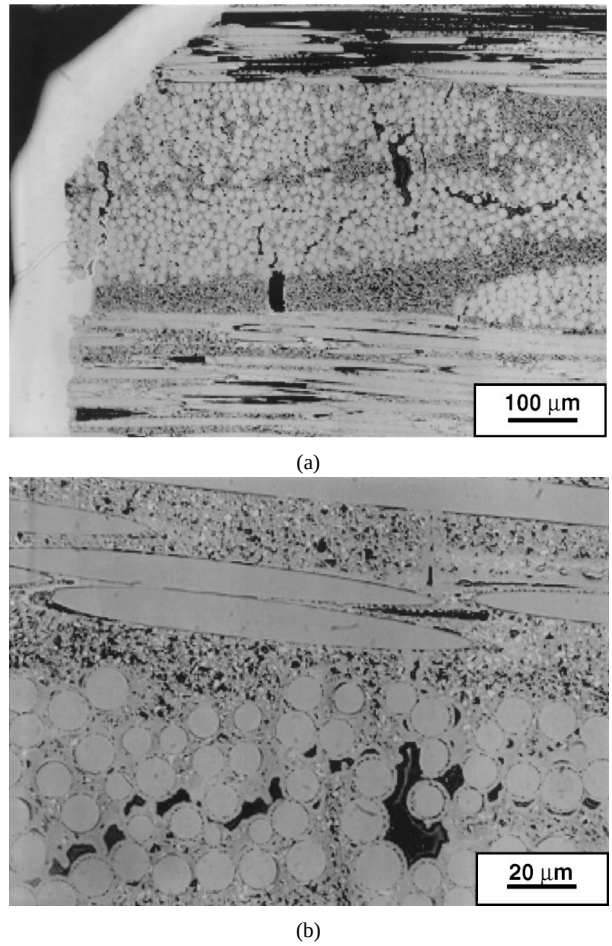

Figure 16 Micrograph of Ceracarb^{TM} material which had been pre-fatigued and thernally fatigued: a) view at 100×, b) view at 500×. No microstructural differences were identified when comparing to as-received material (Fig. 3a and b).

In addition, microscopic inspection also confirmed that there were no notable differences in the microstructures of the pre-conditioned and the thermally tested material compared to the as-received material. Representative micrographs of the pre-conditioned and thermally tested material are shown in Fig. 16. Refer to Fig. 3a and b for comparison micrographs of as-received material.

This evidence may imply that when there is no applied stress during the thermal exposure to open matrix cracks and thus to allow for oxidation ingress at the elevated and intermediate temperatures, the effect is not as pronounced. It may also show that the self-sealing mechanism created by constituents in the matrix material may be extremely effective, even when the exterior composite coating is cracked, at the elevated temperatures.

4.2. Nickel-based superalloy-Rene'41

Tensile properties obtained for the Rene'41 specimens tested are presented in Table III. The strength of the material in the as-received condition was 979 MPa. The modulus and strain to failure for the as-received material were 176 GPa and 64.0%, respectively. After being heat treated at 1093°C for 30 hours, the average room temperature strength and modulus of the material increased while the strain to failure significantly decreased. The values pertaining to the respective

TABLE III Tensile results from as-received and thermally treated material

Rene'41

Specimen#/test type	UTS (MPa)	Modulus (GPa)	Strain @ fail (%)
As-received			
97-A01	977	188	67.82
97-A10	963	171	66.88
97-A18	996	168	58.20
Isothermal-30 hrs			
97-999	1212	208	29.01
97-A12	1210	207	26.03
97-A23	1223	193	25.21
Thermal fatigue (Tmax = 1093 C, N = 4500)			
97-992 (warped)	982	191	24.17
97-993	1034	209	23.16
97-A16	1077	209	33.16
97-A21	1052	202	33.23

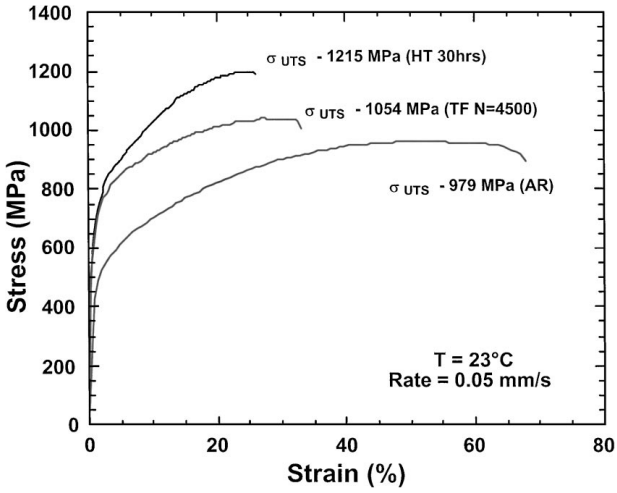

Figure 17 Representative stress vs. strain traces for Rene'41 in the as-received, heat treated, and thermal fatigued condition, respectively.

properties following heat treatment were 1215 MPa, 203 GPa, and 26.8%. The average strength, modulus, and strain to failure for the specimens that were thermally fatigued were measured to be 1054 MPa, 207 GPa, and 29.9%, respectively.

A representative stress-strain curve from each of the test conditions is shown in Fig. 17. The plot illustrates the differences in the properties described above, demonstrating that the behavior of the Rene'41 is dependent on the thermal test conditions. The as-received material showed the lowest ultimate strength, the lowest yield strength and the largest amount of strain to failure. The curves representative of the thermal fatigue and heat treated condition both showed higher yield and ultimate tensile strengths and lower strains to failure compared to the as-received material. Although the shape of the curves for the two treated materials were similar, the heat treated material showed higher ultimate strength.

The differences in behavior between the as-received and thermally treated materials as shown in Fig. 17 illustrates that this alloy is not thermally stable for long or multiple exposures at 1093°C. This temperature is slightly above the original solution heat treatment for the as-received material and thus allowed for a number

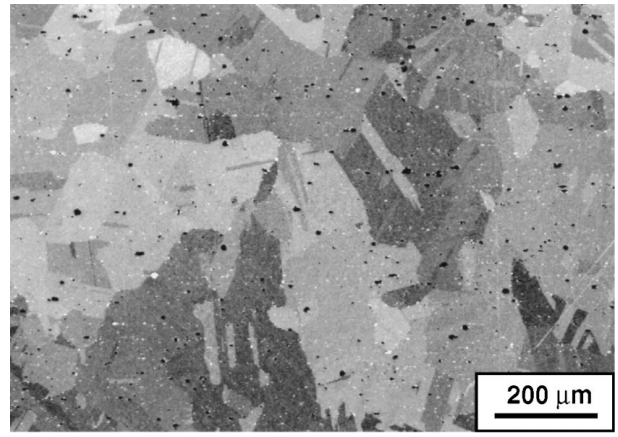

Figure 18 SEM micrograph taken at 100× which shows the microstructure of the nickel-based superalloy Rene'41 after heat treatment for 30 hours at 1093°C. The specimen was prepared using a chromate electropolish.

of microstructural changes. The extended time at temperature most likely dissolved all of the γ', dissolved some of the carbides, and allowed for grain growth [14, 16]. After heat treatment, the samples were air cooled. The air cooling allows for fine gamma prime formation which accounts for the increase in strength and the decrease in ductility. Refer to Figs 4 and 18 for micrographs of the Rene'41 material in the as-received and the heat treated condition, respectively. These micrographs illustrate some of the microstructural changes observed. The general content of the inter- and intragranular carbides seems to have remained unchanged. However, the average ASTM grain size in the as-received material was in the 7 to 8 range, while the ASTM grain size after heat treatment was approximately 3.

The thermal fatigue tests produce an effect similar to the heat treatment, only less time was spent at maximum temperature. In conducting the thermal cycling, the Rene'41 was cycled above and below the solution heat treat temperature. It is suggested that some of the gamma prime should dissolve back into solid solution, and then precipitate into fine particles upon cooling. This would produce a dual structure of fine and blocky gamma prime which would act to increase strength and decrease the strain to failure compared to the as-received material.

Isothermal exposure as well as thermal fatigue at 1093°C also allowed for another change in the Rene'41 structure, the formation of an oxide layer on the outer surface. Fig. 19 shows a micrograph of the cross section near the exposed surface of a Rene'41 sample that had been heat treated for 30 hours at 1090°C. A region of intergranular attack was observed below the surface oxide layer. A needle-like phase was also observed in the region below the oxide. Many nickel-based superalloys are sensitive to intergranular oxidation during extended time at or above the solutionizing temperature.

All of these thermally induced changes observed reduce ductility and promote cracking. The changes in the microstructure would presumably have a pronounced effect under the thermal conditions in the afterburner section of the exhaust nozzle.

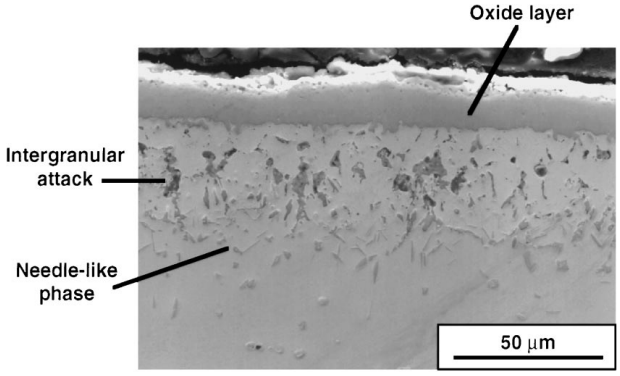

Figure 19 SEM micrograph taken at 750× which illustrates some of the microstructural changes observed after heat treatment: the oxide layer formation on the surface, the region of intergranular attack and the needle-like phases below the surface oxide layer.

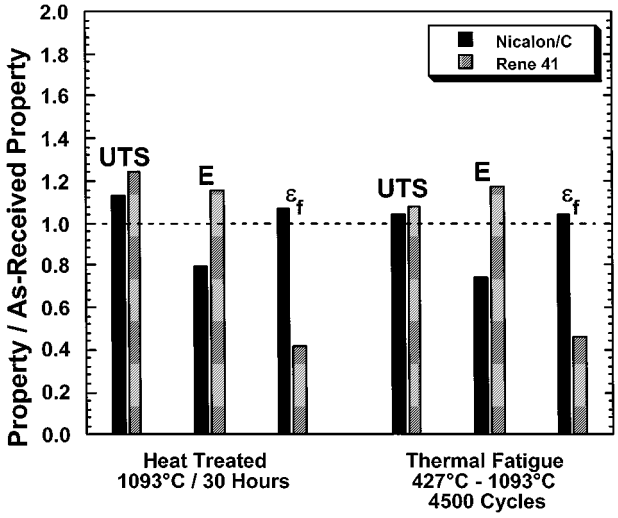

Figure 20 The residual strength data after heat treatment and thermal fatigue for each material were normalized by the respective as-received values and plotted for comparison.

4.3. Discussion

The durability of the Ceracarb^{TM} material was compared to the current exhaust nozzle component material, Rene'41. The residual strength data after heat treatment and thermal fatigue for each material were normalized by the respective as-received values and plotted in Fig. 20. The Ceracarb^{TM} material suffered no loss in strength from the as-received condition, but did see a decrease in modulus. The decrease in modulus was discussed earlier and was attributed to the increased density of matrix cracks imparted by the mechanical pre-conditioning fatigue and not due to the heat treatment or the thermal cycles. Strain to failure for the CMC was slightly larger than unity, indicating that the material experienced a slight increase in toughness as a result of the thermal conditioning. No significant change in tensile properties from the isothermal exposure or from the thermal fatigue suggests that the Ceracarb^{TM} material does not degrade under the time at temperature conditions nor the thermal fatigue conditions tested in this study.

The data obtained from the Rene'41 material showed that the material undergoes significant changes due to the conditions tested. The mean retained strength for both the heat treated and the thermally fatigued Rene'41 was greater that the mean strength measured for the as-received condition. The same is true for the normalized modulus. The strain at failure, however, showed a significant decrease of approximately 60% from the as-received condition. Thus, the material suffered a large drop in toughness, which was also illustrated in the stress-strain curves shown for each condition in Fig. 17. It is this loss in ductility can contribute to cracking of this material when it is used in turbine engine exhaust nozzle applications.

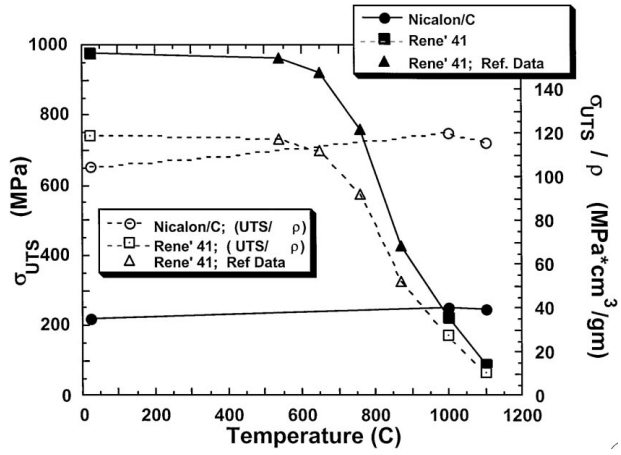

Figure 21 Plot of the ultimate tensile strength (UTS) and specific strength as a function of temperature for both Ceracarb^{TM} and Rene'41. Rene'41 data between 600 and 900°C are found in reference [15].

From this laboratory comparison of properties following heat treatment and thermal fatigue, it appears that both the Ceracarb^{TM} composite and the Rene'41 retain sufficient strength for exhaust nozzle applications. However, performance under load at temperature, which is more typical of real application, separates the two materials. The basic tensile properties of Ceracarb^{TM} at 23, 1000, and 1100°C were determined in an earlier investigation [4, 5]. In order to provide a direct comparison between the CMC and the nickel-base superalloy, tension tests at these temperatures were also generated on Rene'41 samples.

The results of the tension tests are shown in Fig. 21. This figure shows the strengths and the specific strengths of both materials in terms of test temperature. It should be noted that the trace for the Rene'41 material also contains data from reference [15] for strength at temperatures between 600 and 900°C. At room temperature, the Rene'41 was almost five times stronger then the Ceracarb^{TM} material. However, at 1000°C they were approximately equally as strong. At temperatures above 1000°C, Ceracarb^{TM} was substantially stronger. If one looks at the normalized data, the two materials are nearly identical up to 600°C, after which the Ceracarb^{TM} material is significantly superior to the Rene'41. At 1100°C the strength of the Ceracarb^{TM} material is approximately three times greater than the Rene'41.

5. Conclusions

Results from this study illustrated that the Ceracarb^{TM} CMC retained its as-processed strength after mechanical and thermal testing in the laboratory. When exposed

to the same test conditions, Rene'41 also showed no loss in strength but was shown to sacrifice toughness after the thermal exposure. The Ceracarb^{TM} material did not undergo any detrimental changes in microstructure that could be seen optically, or measured mechanically, illustrating the effectiveness of the material's coating system. The Rene'41, on the other hand, showed microstructural instability at the test temperatures causing the change in properties. Since testing was done to isolate only effects of prior mechanical loading, isothermal, and thermal fatigue conditions without being under load, both the CMC and the superalloy appeared to retain desirable properties. However, testing conditions under loads similar to those experienced in application might exemplify the benefits of the thermal stability of the Ceracarb^{TM} over Rene'41.

References

1. D. M. DAWSON, in "High Performance Materials in Aerospace," edited by H. M. Flower (Chapman & Hall, London, 1995) p. 183.
2. R. LEHMAN, in "Structural Ceramics—Treatise on Material Science and Technology," edited by J. B. Watchman (Academic Press Inc., Boston, 1989) p. 229.
3. R. N. KATZ, in "Structural Ceramics—Treatise on Material Science and Technology," edited by J. B. Watchman (Academic Press Inc., Boston, 1989) p. 10.
4. L. P. ZAWADA and S. S. LEE, Presented at Advance Research Projects Agency Ceramic Insertion Program Annual Review, (Annapolis, 1994).
5. L. P. ZAWADA, Presented at Advanced Research Projects Agency Ceramic Insertion Program Review, (Annapolis, 1997).
6. K. K. CHAWLA, "Ceramic Matrix Composites" (Chapman and Hall, New York, 1993).
7. T. ARAKI, T. NATUMURA, M. HAYASHI, S. SUGAI, *et al*., in Proceedings of the 4th Japan International SAMPE Symposium, (Japan, 1995) p. 374.
8. P. SPRIET, D. BOURY and G. HABAROU, in "High Temperature Ceramic-Matrix Composites I: Design, Durability, and Performance, edited by A. G. Evans and R. Naslain" (American Ceramic Society, Westerville, 1995) p. 191.
9. P. SPRIET and G. HABAROU, in Proceedings of the 1st International Conference on Ceramic and Metal Matrix Composites, CMMC'96 Part 2 (of 2), (Spain, 1996) p. 1267.
10. L. HERAUND, in Proceedings of the Verbundwerk (1990) p. 25.21.
11. A. K. GOPALAN, J. A. MANTEIGA and J. C. MAYER, in The Leading Edge, Winter, 12–15.
12. http://www.cnn.com/US/9904/27/F16.crash (1999).
13. *Armed Forces Journal International* (1996) 20.
14. "Superalloys: A Technical Guide" edited by E. F. Bradley (ASM International, Metals Park, 1988) p. 163.
15. Metals Handbook, "Properties and Selection: Stainless Steels, Tool Materials, and Special Purpose Metals" vol. 3 (ASM International, Metals Park, 1980) p. 208.
16. C. T. SIMS, N. S. STOLOFF and W. C. HAGEL, "Superalloys II—High Temperature Materials for Aerospace and Industrial Power" (John Wiley and Sons, New York, 1987) p. 591, 598, 604.
17. M. HUGER, S. SOUCHARD and C. GAULT, *J. Mater. Sci. Let.* (1993) 414.
18. R. NASLAIN, in Proceedings of the Second International Conference on High-Temperature Ceramic-Matrix Composites II: Manufacturing and Materials Development, edited by A. G. Evans and R. Naslain (The American Ceramic Society, Santa Barbara, 1995) p. 23.
19. G. N. MORSCHER, D. BRYANT and R. E. TRESSLER, in Proceedings of edited
20. J. D. CAWLEY, A. J. ECKEL and T. A. PARTHASARATHY, in Proceedings of edited
21. A. E. EVANS, F. W. ZOK and R. M. MCMEEKING, *J. Am. Ceram. Soc.* (1996) 2345.
22. S. C. SCHWARTZ, S. LEE and P. V. MOSHER, in "Damage and Oxidation Protection in High Temperature Composites" (American Society of Mechanical Engineers, New York, 1991) p. 23.
23. X. BOURRAT, K. S. TURNER and A. E. EVANS, *J. Am. Ceram. Soc.* (1995) 3050.
24. ASTM Subcommittee C28.07 on Ceramic Matrix Composites, (Philadelphia, 1994).
25. E. LARA-CURZIO, M. K. FERBER, R. BOISVERT and A. SZWEDA, in Proceedings of the 19th Annual Conference on Composites, Advanced Ceramics, Materials, and Structures—B, (American Ceramic Society, Cocoa Beach, 1995) 341.
26. S. S. LEE, L. P. ZAWADA, R. HAY and C. FOLSOM, *J. Am. Ceram. Soc.* (1998) in press.

Received 22 June
and accepted 23 November 1999